JMEPEG
https://doi.org/10.1007/s11665-025-11096-7

1059-9495/$19.00

ORIGINAL RESEARCH ARTICLE

Optimizing Cold Spray Deposition on Thermoplastics: A Machine Learning Approach Focused on Powder Properties

Alessia Serena Perna, Alessia Auriemma Citarella, Fabiola De Marco, Luigi Di Biasi, Antonio Viscusi, Genoveffa Tortora, and Massimo Durante

Submitted: 3 December 2024 / Revised: 14 February 2025 / Accepted: 3 March 2025

The cold spray (CS) process offers an advanced method for metallizing thermoplastic polymers, providing a low-temperature solution to overcome the limitations of traditional coating techniques. However, optimizing the cold spray process for metallizing thermoplastic polymers is a complex task due to the numerous interacting parameters that influence coating quality. As traditional trial-and-error approaches are time-consuming and costly, machine learning (ML) could offer a solution to these challenges by providing further insights into the process and enabling more efficient optimization. The aim of this work is to identify the most relevant input parameters for ML models, with a particular focus on powder characteristics, to predict two critical outcomes: particle flattening and penetration depth. Two distinct datasets were created for this study: one focused on particle yield strength and the other on powder density, each combined with further input parameters like impact velocity and substrate yield strength. These datasets were constructed using experimental data and finite element modeling (FEM) simulations, with materials including copper, aluminum, titanium, and others, applied to thermoplastic substrates like polyether ether ketone (PEEK), acrylonitrile butadiene styrene (ABS), and polyamide 66 (PA66). Several ML algorithms, including decision trees, neural networks, and Gaussian process regression, were tested to predict coating behavior, and the effects of Z-score normalization were evaluated for improving model stability and prediction accuracy. The results show that particle yield strength is crucial for flattening, while particle density primarily governs penetration depth. This study demonstrates that ML, when combined with a solid understanding of the process, offers an effective framework for optimizing CS deposition on polymers.

Keywords cold spray, machine learning, metallic powders, polymers and plastics

This article is an invited paper selected from presentations at the 5th International Symposium on Dynamic Response and Failure of Composite Materials, held June 17–21, 2024, in Island of Ischia, Italy, organized by Prof. Valentina Lopresto, Dr. Ilaria Papa, Prof. Michele Guida, and Prof. Antonello Astarita, University of Naples Federico II. It has been expanded from the first presentation and peer reviewed as an original paper following the standard procedure of the journal.

Alessia Serena Perna and **Massimo Durante**, Department of Chemical, Materials and Production Engineering, University of Naples "Federico II", P.le Tecchio 80, 80125 Naples, Italy; **Alessia Auriemma Citarella, Fabiola De Marco, Luigi Di Biasi,** and **Genoveffa Tortora**, Department of Computer Science, University of Salerno, Fisciano, Salerno, Italy; **Antonio Viscusi**, Department of Chemical, Materials and Production Engineering, University of Naples "Federico II", P.le Tecchio 80, 80125 Naples, Italy; and Faculty of Technology and Innovation Sciences, Universitas Mercatorum, Piazza Mattei 10, 00186 Rome, Italy. Contact e-mail: alessiaserena.perna@unina.it.

1. Introduction

Thermoplastic polymers have experienced significant growth in both research and industry due to their exceptional properties, such as high strength, toughness, chemical resistance, and ease of processing (Ref 1-3). A major factor fuelling this interest is the increasing demand for sustainable and recyclable materials (Ref 4). As industries seek to reduce their environmental footprint, thermoplastics offer a promising solution compared to traditional thermosetting polymers, which cannot be remelted and reformed (Ref 5, 6). This adaptability has led to advancements in high-performance thermoplastics, particularly in industries that require materials capable of withstanding extreme conditions (Ref 7). Materials like polyether ether ketone (PEEK), polyphenylene sulfide (PPS), and polyimides (PI), AND Acrylonitrile butadiene styrene (ABS) are notable for their excellent thermal stability, increasingly replacing metals and traditional thermosets in demanding applications (Ref 8, 9). The rise of additive manufacturing has also driven innovation, allowing high-performance thermoplastics to be customized for 3D printing, enabling complex geometries and tailored material properties (Ref 1). However, despite their advantages, thermoplastics are still limited by issues such as lower surface hardness, susceptibility to scratching and wear, and inadequate resistance to UV light and chemicals (Ref 10, 11). Additionally, thermoplastics often lack the electrical and thermal conductivity required in certain

Published online: 28 March 2025

applications, posing challenges in fields that demand efficient heat dissipation or electrical grounding (Ref 12).

To address these limitations, surface modification techniques, such as metallization, have become increasingly important (Ref 13). Traditional techniques, like thermal spray methods, pose considerable risks to polymer surfaces, as their high temperatures can cause thermal degradation, distortion, or damage (Ref 14). Additionally, vapor deposition techniques, while capable of producing thin, uniform coatings, tend to be expensive, slow, and suitable only for small workpieces due to vacuum requirements (Ref 15). In contrast, cold spray (CS) technology has emerged as an effective alternative for metallizing polymers (Ref 16, 17). CS is a low-temperature process in which metallic powders are accelerated to supersonic speeds and impact a substrate, forming strong bonds without thermal degradation (Ref 18). This makes it particularly useful for coating temperature-sensitive materials like thermoplastics, avoiding the thermal damage associated with traditional thermal spray methods (Ref 19). Furthermore, cold spray avoids harmful chemicals and high vacuum requirements, reducing environmental impact and operational costs (Ref 20). Cold spray has been successfully used to apply a wide range of metallic coatings, including aluminum, copper, and steel, on various substrates, such as thermoplastics, polymers, and composites, leading to improved performance and durability (Ref 21-23). Its application to polymer substrates offers promising opportunities across various fields. In aerospace, cold spray coatings could enhance the lightning strike protection of lightweight composites like CFRPs and PEEK, improving their electrical conductivity while maintaining structural integrity (Ref 24). In the automotive sector, cold spray could enhance the thermal stability, wear resistance, and EMI shielding of plastic and composite parts, particularly in electric vehicles (Ref 25). Biomedical applications include coatings for prosthetic implants and medical devices, where biocompatible materials such as titanium and hydroxyapatite could improve osseointegration and wear resistance (Ref 26). Most of these studies are based on experiments, and while metal-to-metal deposition has been modeled theoretically and numerically, advanced modeling for deposition on polymeric and composite materials is lacking. The few numerical models developed tend to be inefficient, requiring extensive calculations of numerous parameters related to both the particles and the substrate, which often makes material characterization more burdensome than the experimental deposition tests (Ref 27, 28).

In this context, machine learning (ML) offers a cost-effective solution to enhance cold spray technology for polymer metallization by minimizing the need for extensive experimental tests with various powders or substrates. The integration of ML techniques into cold spray processing could further accelerate its implementation by enabling the prediction of coating characteristics, reducing the reliance on extensive experimental testing or complex numerical modeling. An ML-driven approach could aid in selecting optimal polymer substrates and fine-tuning process parameters to achieve desired coating properties. Previous studies have highlighted the potential of ML techniques to predict cold spray coating characteristics (Ref 29, 30). However, since these characteristics depend on numerous factors related to both the process and the materials, further research is necessary to identify the most relevant parameters to include as inputs for the models. These input parameters can be grouped into three main categories: process parameters, substrate parameters, and powder parameters. To keep the model manageable, it is crucial to limit the number of parameters selected from each category (Ref 31).

This study aims to leverage machine learning techniques to predict and optimize the CS deposition on thermoplastic polymers. The focus is on identifying the most influential parameters that govern coating uniformity and adhesion on the substrate. Specifically, this research investigates the impact of two key powder characteristics, yield strength and density, on the model's ability to predict effective coating results. In addition to the powder characteristics, impact velocity, which encompasses key process parameters was included, along with the yield strength of the substrate, chosen for its role in governing plastic deformation during deposition. The output parameters considered were penetration depth, which measures how deeply the particles embed into the substrate, and flattening, which describes the extent to which particles deform and spread upon impact. To ensure the model was trained on a sufficiently large and accurate dataset while minimizing potential inaccuracies, a hybrid approach was adopted, combining experimental data with computational data derived from finite element models (FEM). To build the dataset, a variety of metallic materials were considered for both the experimental trials and the FEM simulations. The powders selected included copper, aluminum, titanium, 316L steel, and Inconel 718, while different polymeric substrates, such as PEEK, ABS, and PA66, were used for deposition. For the machine learning experiments, the MATLAB Classifier Learner app was employed, utilizing a range of algorithms to ensure comprehensive testing and performance evaluation. By leveraging both computational approaches and existing knowledge of the process, this study seeks to enhance the understanding of how various parameters influence coating quality, ultimately contributing to more efficient and informed process optimization.

2. Materials and Methods

2.1 Composition of the Dataset

In this study, two distinct datasets were used, each defined by different input parameters while sharing the same output parameters. To evaluate the influence of powder characteristics, the first dataset, referred to as the "Yp dataset," included the yield strength of the powders (Yp), particle impact velocity (v_p), and substrate yield strength (Ys) as its input parameters. The second dataset, labeled the "ρ dataset," utilized powder density (ρ), particle impact velocity (vp), and substrate yield strength as the input parameters.

The selection of Yp and ρ as the powder properties for comparison stems from their significance in the cold spray literature and their critical influence on the deposition process (Ref 32, 33). Yield strength is a pivotal factor in determining the degree of plastic deformation experienced by the powders during impact, while density integrates particle size and mass, offering insight into particle acceleration dynamics.

In addition to the powder characteristics, other input parameters included impact velocity and yield strength of the substrate. The first was included as a key process parameter because it reflects the combined effects of temperature, pressure, and standoff distance, all of which directly influence the deposition process (Ref 34). The latter was considered as it governs the plastic deformation of the substrate during particle impact (Ref 35).

The output parameters evaluated were penetration depth and flattening, both of which are essential for assessing coating adhesion in cold spray processes. Penetration depth quantifies the extent to which particles embed into the substrate and is influenced by factors, such as impact velocity, particle temperature, and material properties (Ref 36, 37). Flattening describes the degree of deformation and spreading of particles upon impact, which depends on variables like particle velocity, temperature, size, and substrate characteristics. These metrics, critical for understanding coating adhesion in cold spray processes, are defined in Eq 1 and 2:

$$Flattening[\%] = \frac{d_p - d_{p,i}}{d_p} \times 100 \qquad \text{(Eq 1)}$$

$$Penetration\ depth[\%] = \frac{H_s - H_{s,i}}{H_s} \times 100 \qquad \text{(Eq 2)}$$

where d_p and H_s represent the particle diameter and substrate height before impact, $d_{p,i}$ and $H_{s,i}$ denote these parameters after impact.

To ensure the reliability of the machine learning models, a large and accurate dataset was required. A hybrid approach was adopted, combining a limited amount of experimental data with computational data generated through finite element modeling (FEM). Although FEM data may lack the precision of experimental measurements, they address the practical limitations of experimental studies. Accordingly, the datasets were composed of 30% experimental data and 70% FEM data. Each dataset contained a total of 198 samples, which were equally divided for analysis, with 99 samples allocated for training the models and the remaining 99 used for testing and evaluating model performance. The materials selected for the datasets were chosen based on their diverse properties and relevance to cold spray applications. The powders analyzed included copper, aluminum, 316 steel, titanium, Inconel718, and tin, while the substrates used in the study comprised PEEK, ABS, and PA66. The characteristics of the tested materials, based on previous experiments and literature (Ref 38, 39), are presented in Table 1, for the powder, and Table 2, for the substrates.

Experimental data were gathered analyzing the coatings obtained by employing low-pressure cold spray equipment (DYCOMET), considering all the evaluated substrates and powders. For the remaining 70% of the dataset, a finite element model was developed to simulate the impact of a single metallic particle on a polymeric substrate using a commercially available FE analysis program (Abaqus). For the machine learning experiments, the MATLAB Classifier Learner app was utilized to explore a diverse array of algorithms, enabling thorough testing and assessment of model performance. Various approaches, such as linear classifiers (Ref 40), decision trees (Ref 41), ensemble techniques (Ref 42), and support vector machines (Ref 43), were systematically evaluated to identify the most effective predictive models. In this study, only the top-performing algorithms are reported in the results. To evaluate the robustness of the models, k-fold cross-validation using both $k = 5$ and $k = 10$ were conducted. Given the relatively small dataset size, it was found that the results were equivalent across both values of k, indicating stable model performance.

2.2 FEM Modeling for Training Dataset Construction

A finite element (FE) model was developed using Abaqus to simulate the high-velocity impact of a single metallic particle on a polymeric substrate, aiming to ensure the accuracy of the training dataset. The FE model was previously validated, providing reliable predictions for material deformation under diverse impact conditions (Ref 44). The simulation used a 2D-axisymmetric Lagrangian framework, commonly applied in high-impact studies, to model a spherical particle impacting perpendicularly onto a substrate at least five times its size (Ref 45-47). This size ratio was selected to prevent interference from reflected elastic waves at the boundaries during impact. The particle diameter was set to 18 μm, and the computational domain featured a finely graded mesh, with the particle and the interface region of the substrate sharing a nominal element size of 18 μm/25. Dynamic explicit analysis accounted for adiabatic heating effects, while boundary constraints were applied to the substrate. Initial conditions included the particle's velocity and a room temperature of 298 K for both components. Gravity and air resistance were neglected, but plasticity-induced heating and frictional effects (with a coefficient of 0.35) were incorporated using the general contact algorithm (Ref 48). Material behavior followed the Johnson-Cook (JC) plasticity model, suitable for large strains, high strain rates, and thermal softening. The JC model parameters were integrated into simulations involving

Table 2 Substrates properties used for the construction of the training and test datasets

Material parameters	PEEK	ABS	PA66
Density, kg/m^3	1300	1040	1140
Yield Strength, GPa	0.141	0.045	0.054
Young's modulus, GPa	3.5	2.3	2.9
Poisson ratio	0.4	0.32	0.42
Thermal conductivity, W/m °C	0.25	0.16	0.2
Heat capacity, J/kg °C	2180	2100	1500
Melting temperature, °C	341	240	257

Table 1 Powder properties used for the construction of the training and test datasets

Material parameters	Copper	Aluminum	316L steel	Titanium	Tin	Inconel718
Density, kg/m^3	8960	2710	8000	4500	5765	8190
Yield Strength, GPa	0.033	0.18	0.29	0.97	0.017	1.035
Young's modulus, GPa	124	68.9	193	109	44.3	194.6
Poisson ratio	0.34	0.33	0.25	0.338	0.33	0.30
Thermal conductivity, W/m °C	386	204	16.2	21.4	63.2	11.4
Heat capacity, J/kg °C	383	904	500	520	213	435
Melting temperature, °C	1083	630	1371	1650	231.9	1300

different material combinations of the metal particles and polymeric substrates. In addition to the material properties outlined in Tables 1 and 2, the simulations incorporated supplementary parameters, as specified in Tables 3 and 4.

Output parameters of particle flattening and penetration depth were calculated for velocities ranging from 50 to 350 m/s in 30 m/s increments for each material combination, according to Eq 1 and 2.

2.3 Cold Spray Deposition for Training and Test Dataset Construction

The substrates were composed of thermoplastic panels measuring 100 mm × 100 mm × 5 mm. Micron-sized spherical metallic powders, provided by LPW South Europe, with diameters ranging from 10 to 40 μm, were sprayed onto the thermoplastic surface using the cold spray process. The particle size distribution of the powders used is detailed in the authors' previous works (Ref 23, 49). The metallization was conducted using a low-pressure cold spray (LPCS) machine (Dycomet 423), with nitrogen serving as the propellant gas. In this study, carrier gas pressure, standoff distance, and temperature were varied, as they significantly influence impact velocity in cold spray deposition (Ref 50, 51). Although gas pressure is not the primary factor affecting deposition on polymer substrates, since impact velocity can also be effectively controlled by modifying standoff distance and temperature (Ref 52), it was regulated within the machine's operating range to achieve more precise tuning of the deposition process. Standoff distance is a critical parameter, as shorter distances result in greater thermal exposure and increased impact pressure from particle collisions, influencing the coating growth mechanism (Ref 53, 54). Proper optimization of this parameter is essential for enhancing deposition efficiency while mitigating issues such as delamination and erosion. The temperature at the nozzle outlet was monitored using a K type thermocouple. In CS deposition on polymer substrates, careful temperature selection is crucial to prevent thermal degradation, as these materials are highly sensitive to elevated temperatures. The gun traverse speed was maintained at 1.6 mm per second to ensure sufficient substrate heating, facilitating the effective accommodation of impacting particles (Ref 55). The selected process parameters were based on prior research and established literature (Ref 56-62) and are summarized in Table 5.

The samples were positioned on a platform. The spraying gun, mounted on a HIGH-Z S-400/T-CNC-Technik robot, operated remotely and sprayed perpendicularly to the substrates. For evaluating impact velocity, models from the literature were employed to calculate this parameter based on the processing conditions (Ref 33, 50). After deposition, the coating characteristics selected as output parameters, namely flattening and penetration depth, were assessed. To measure these values, the specimens were sectioned perpendicular to the coating surface, and the surfaces were analyzed using a Hitachi TM3000 electron microscope (Fig. 1). SEM micrographs were analyzed using Fiji software, with a custom script developed to automate particle recognition and measurement. A thresholding technique was applied to enhance the contrast between metallic particles and the polymeric substrate, thereby facilitating accurate measurement. For each dataset entry, five micrographs, each measuring 500 × 500 μm, were analyzed to determine the mean values of flattening and penetration depth. Flattening was calculated as the percentage change in particle diameter following impact, with the measurement averaged over ten particles per micrograph. Similarly, penetration depth was quantified as the ratio of the change in substrate height to its initial height, based on ten measurements per micrograph to ensure the reliability and consistency of the results.

2.4 Machine Learning Models

The range of ML models present in MATLAB Classifier Learner app were tested to predict key output variables of the

Table 4 Substrates properties used in the FEM simulations

Material parameters	PEEK	ABS	PA66
Yield strength, A, MPa	132	39	110
Hardening modulus, B, MPa	10	48	0
Hardening exponent ,n	1.2	1.5	1
Strain rate sensitivity coefficient, C	0.034	0.053	0.01
Reference strain rate, ε_0°, s^{-1}	0.001	0.001	0.001
Thermal exponent, m	0.634	0.88	0.8
Inelastic heat fraction	0.9	0.9	0.9
Reference temperature, T_R,, °C	143	97	140

Table 5 Process parameters employed for CS deposition

Temperature in the process chamber, °C	25
Temperature at the outlet of the nozzle, °C	100-350
Velocity at the nozzle outlet, mm/s	1.6
Carrier gas inlet pressure, MPa	0.6-0.8
Standoff distance, mm	20-100

Table 3 Powder properties used in the FEM simulations

Material parameters	Copper	Aluminum	316L steel	Titanium	Tin	Inconel718
Yield strength, A, MPa	90	148.4	305	88.36	45.50	1108
Hardening modulus, B, MPa	292	345.5	1161	783.54	267.73	699
Hardening exponent ,n	0.31	0.183	0.61	0.5009	0.3947	0.5189
Strain rate sensitivity coefficient, C	0.025	0.001	0.01	0.0943	0.0966	0.0085
Reference strain rate, ε_0°, s^{-1}	1.0	1.0	1.0	1	1.0	1.0
Thermal exponent, m	1.09	0.895	0.517	0.4527	0.4560	1.2861
Inelastic heat fraction	0.9	0.9	0.9	0.9	0.9	0.9
Reference temperature, T_R, , °C	298	298	298	298	298	298

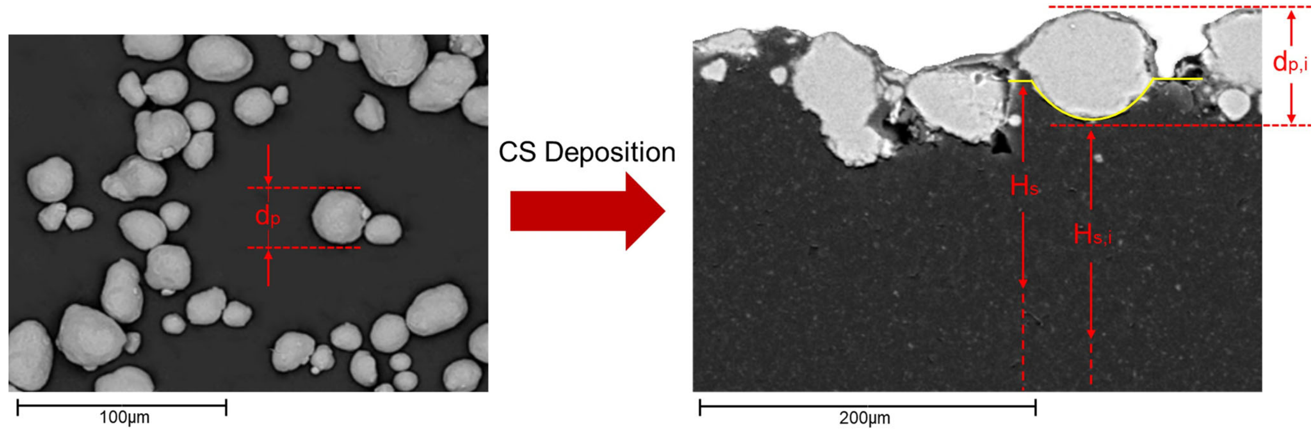

Fig. 1 Scheme illustrating the parameters employed for the calculation of flattening and penetration depth

process. All ML models were implemented and evaluated using MATLAB, utilizing the Classifier Learner app to train and assess the algorithms. The models that exhibited the best performance in predicting flattening and penetration depth were squared exponential Gaussian process regression (GPR), boosted trees, Matern 5/2 GPR, trilayered neural network, and medium neural network. These models were selected for their ability to effectively capture the complex, nonlinear relationships between the input parameters, which included particle yield strength, density, impact velocity, and substrate yield strength. The Squared Exponential GPR model was particularly effective due to its ability to model smooth, continuous relationships in the data. This made it well-suited for predicting output variables with high accuracy. Similarly, the Matern 5/2 GPR model was used for its flexibility, providing robust predictions across a wider range of data patterns, while also offering uncertainty estimates that complemented the predictions. Boosted Trees, specifically gradient boosting models, were selected for their capacity to improve prediction performance by combining the strengths of multiple weak learners into a more powerful and reliable model. The trilayered neural network model was employed for its ability to capture complex, nonlinear interactions in the dataset, allowing it to provide highly accurate predictions for the output variables. Additionally, the medium neural network proved effective by modeling intricate relationships and delivering reliable results across the datasets.

To assess the performance of these models, several evaluation metrics were used: root mean square error (RMSE), R-squared (R^2), mean squared error (MSE), and mean absolute error (MAE). Those parameters are defined in Eq 3-6.

$$RMSE = \sqrt{\left(\frac{1}{n}\right)\sum_{i=1}^{n}(y_i - x_i)^2} \quad \text{(Eq 3)}$$

$$R - \text{squared} = 1 - \frac{\sum_{i=1}^{n} e_i^2}{\sum_{i=1}^{n}(y_i - y)^2} \quad \text{(Eq 4)}$$

$$MSE = \sum_{i=1}^{D}(x_i - y_i)^2 \quad \text{(Eq 5)}$$

$$MAE = \sum_{i=1}^{D}|x_i - y_i| \quad \text{(Eq 6)}$$

The RMSE is a metric sensitive to outliers that calculates the square root of the average squared errors. R^2 quantifies how well the model's predictions align with the observed data in terms of variance. The MSE calculates the average squared differences between predicted and observed values, while the MAE assesses the average absolute differences between predictions and actual outcomes, giving a clearer view of model performance without the influence of outliers. Lower values for these metrics indicate better model accuracy. To improve the models' stability and performance, Z-score normalization was tested. Z-score normalization, also known as standardization, is a statistical technique used to scale the values of a dataset so that they have a mean of 0 and a standard deviation of 1 (Ref 63). It transforms data points to a standard scale, making them easier to compare, while preserving the relationships between the values. The formula for Z-score normalization is:

$$z = (x - \mu)/\sigma \quad \text{(Eq 7)}$$

where x is the original value, μ is the mean (average) of the dataset, σ is the standard deviation of the dataset and z represented the normalized value (Z-score). Z-score normalization is a common preprocessing step in machine learning, ensuring that features are on a comparable scale for better model performance. In MATLAB, Z-score normalization was used to standardize data by centering it (mean = 0) and scaling it (standard deviation = 1).

3. Results and Discussion

The test results for the two distinct datasets are summarized below. For each input parameter (namely, flattening and penetration depth), and based on whether Z-score normalization was applied or not, the performance of the deep learning models yielding the best results is reported. For the Yp-dataset, which uses particle yield strength as the defining parameter for powder characterization, the results are presented in Table 6, where no Z-score normalization has been applied.

Regarding the results obtained for the ρ-dataset, which considers density as the defining parameter for powder characterization, the outcomes without Z-score normalization are presented in Table 7.

Table 6 Performance metrics for the models predicting flattening and penetration depth on the Yp-dataset, evaluated on validation and test sets

Output parameter	Model	Dataset	RMSE	R-Squared	MSE	MAE
Flattening	Squared exponential GPR	Validation set	2.37	0.80	5.63	1.44
		Test set	2.41	− 0.36	5.8	1.68
Penetration depth	Boosted trees	Validation set	1.22	0.84	1.48	0.89
		Test set	3.58	0.40	12.8	2.86

Table 7 Performance metrics for the models predicting flattening and penetration depth on the ρ-dataset, evaluated on validation and test sets

Output parameter	Model	Dataset	RMSE	R-Squared	MSE	MAE
Flattening	Matern 5/2 GPR	Validation set	1.71	0.90	2.91	0.94
		Test set	6.44	− 8.70	41.42	5.25
Penetration depth	Trilayered neural network	Validation set	0.40	0.98	0.16	0.30
		Test set	2.65	0.67	7.03	2.06

It is worth noticing that, for the same output parameter, different models achieve the best performance depending on the dataset considered. To facilitate a clearer comparison of the results obtained, the outcomes are presented in the graph shown in Fig. 2.

It can be observed that, for flattening, the Yp-dataset consistently yields lower error values across all performance metrics, with predictions being up to 86% more accurate. In contrast, for penetration depth, the dataset based on density leads to more accurate predictions for all performance indicators, resulting in a 45% improvement in MSE. To evaluate its potential impact on model performance, stability, and efficiency, Z-score normalization was applied to standardize the feature scales. The results obtained with this normalization for the Yp-dataset are presented in Table 8.

The results obtained for the ρ-dataset, with Z-score normalization applied, are presented in Table 9.

As in previous cases, different models achieved the best performance for predicting flattening and penetration depth. The results are presented in the graphs shown in Fig. 3 to allow for an effective comparison.

A notable improvement is observed in the prediction of flattening for the ρ-dataset, with performance exceeding that of the Yp-dataset, although the difference remains at a maximum of 0.20. In contrast, for the prediction of penetration depth, the Yp-dataset exhibits superior performance. However, to assess whether Z-score normalization contributes to improved results, it is necessary to compare these outcomes with those obtained from the non-normalized data. For ease of comparison, the results are presented in Fig. 4.

A detailed analysis of Fig. 4 demonstrates that normalization significantly reduces the prediction error for flattening. In contrast, for penetration depth, normalization results in a substantial increase in error values across all performance metrics. Such trends are consistent across both datasets. Therefore, it is recommended to apply normalization exclusively when the output parameter being modeled is flattening.

The results reveal distinct advantages and limitations when using yield strength or density as input parameters, with each offering unique insights into the CS process. From an engineering standpoint, yield strength plays a critical role in particle flattening because it governs the material's resistance to plastic deformation. Softer particles with low Yp, such as copper and tin, deform more readily upon impact, leading to greater flattening. This behavior is particularly evident on firmer substrates like PEEK, which provide the necessary mechanical resistance to induce deformation. Conversely, harder particles, such as titanium or Inconel, display limited flattening due to their higher resistance to plastic deformation. On the other hand, density is a more critical parameter for penetration depth because it directly influences the kinetic energy of the particles, which is proportional to mass and velocity squared. Denser particles, like copper, steel and Inconel, retain more momentum and penetrate deeper into the substrate, whereas lighter materials, such as aluminum, exhibit reduced penetration due to their lower energy transfer. Substrate compliance further amplifies these effects, as softer substrates like ABS allow deeper penetration by dissipating kinetic energy more effectively, while firmer substrates resist deformation.

The varying influence of the two input parameters on the considered outputs provides insight into why Z-score normalization reduces prediction error for flattening while leading to an increase in error when predicting penetration depth. Z-score normalization standardizes feature values and is particularly effective in reducing error when the relationship between input and output variables is nonlinear. Since the correlation between the plastic deformation of the particle, and consequently flattening, and its yield strength is highly nonlinear due to strain hardening and the absence of a perfectly rigid substrate, normalization enables the model to capture subtle variations more effectively, thereby enhancing prediction accuracy (Ref 33, 36). The correlation between penetration depth and particle density is predominantly linear. Specifically, the particle's ability to penetrate the substrate depends on the latter's capacity for plastic deformation. By considering the substrate deformation as the impact of a sphere on a plane, in accordance with Hertz's theory, the energy required for substrate deformation can be expressed as follows (Ref 33):

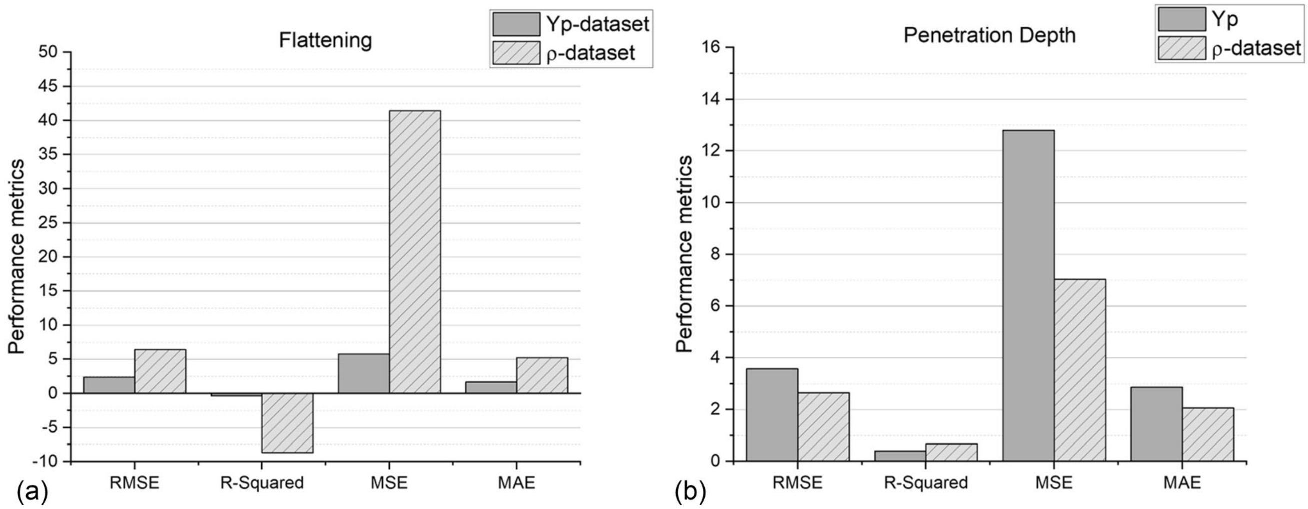

Fig. 2 Comparison of performance metrics for Yp-dataset and ρ-dataset, evaluated for (a) Flattening and (b) Penetration Depth

Table 8 Performance metrics for the models predicting flattening and penetration depth on the Yp-dataset, evaluated on validation and test sets with Z-score normalization applied

Output parameter	Model	Dataset	RMSE	R-Squared	MSE	MAE
Flattening	Squared exponential GPR	Validation set	0.46	0.78	0.22	0.27
		Test set	1.26	− 0.61	1.60	1.05
Penetration depth	Trilayered neural network	Validation set	0.38	0.85	0.15	0.24
		Test set	5.37	− 28.11	28.84	3.61

Table 9 Performance metrics for the models predicting flattening and penetration depth on the ρ-dataset, evaluated on validation and test sets with Z-score normalization applied

Output parameter	Model	Dataset	RMSE	R-Squared	MSE	MAE
Flattening	Squared exponential GPR	Validation set	0.32	0.90	0.10	0.19
		Test set	1.19	− 0.43	1.42	0.81
Penetration depth	Medium neural network	Validation set	0.22	0.95	0.05	0.11
		Test set	6.62	− 43.22	43.82	5.54

$$E_{\mathrm{PLA}} = \left(\frac{\pi a^{*4} 3 Y_s}{4R}\right) = Vp3Y_s \quad \text{(Eq 8)}$$

where Ys represents the yield strength of the substrate, and $\pi a^{*4}/4R$ corresponds to the apparent volume of the particle, which is the volume of material displaced upon impact. This displaced volume closely approximates the particle's volume (Vp) when complete penetration into the substrate occurs. Considering that the kinetic energy, which is the primary form of energy possessed by the particle as it exits the nozzle, is given by $E_k = \rho V_p v^2$, it follows that the relationship between substrate deformation and particle density is largely linear, assuming the impact velocity, controlled through process parameters, remains constant. The disparity between validation and test results highlights the need for more robust training datasets and models that better capture complex, nonlinear relationships. While Z-score normalization effectively stabilized feature scales, leading to improved convergence and reduced training instability, the results indicate that preprocessing alone is insufficient to address the inherent challenges of modeling flattening behavior, particularly for softer particles or lower velocities.

From a machine learning perspective, the selection of input parameters significantly impacts model performance. Yield strength, which captures the material's deformation behavior, is a more suitable predictor for flattening. However, the results indicate that models using Yp struggled to generalize on test sets, suggesting that flattening is influenced by complex, nonlinear factors, such as strain hardening and substrate interaction. Gaussian process regression (GPR) performed best in predicting flattening because it is particularly adept at capturing smooth but nonlinear relationships. GPR is a nonparametric, probabilistic model that excels in situations where the underlying function is not strictly linear. It works by inferring a distribution over possible functions, making it well-suited for predicting complex, nonlinear behavior in the

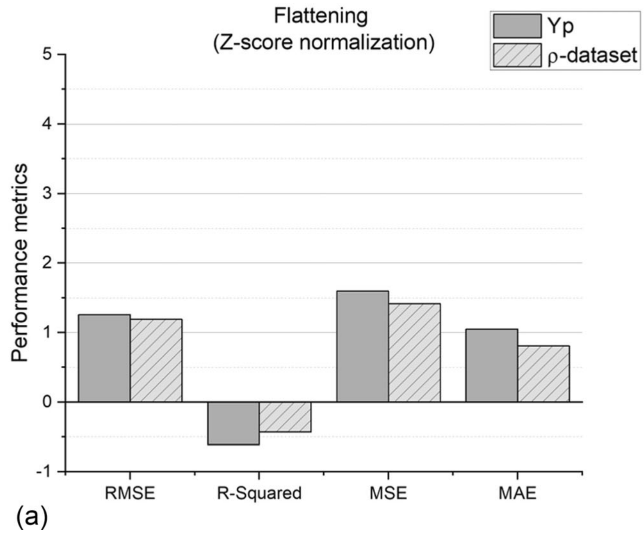

Fig. 3 Comparison of performance metrics for Yp-dataset and ρ-dataset with Z-score Normalization Applied, evaluated for (a) Flattening and (b) Penetration Depth

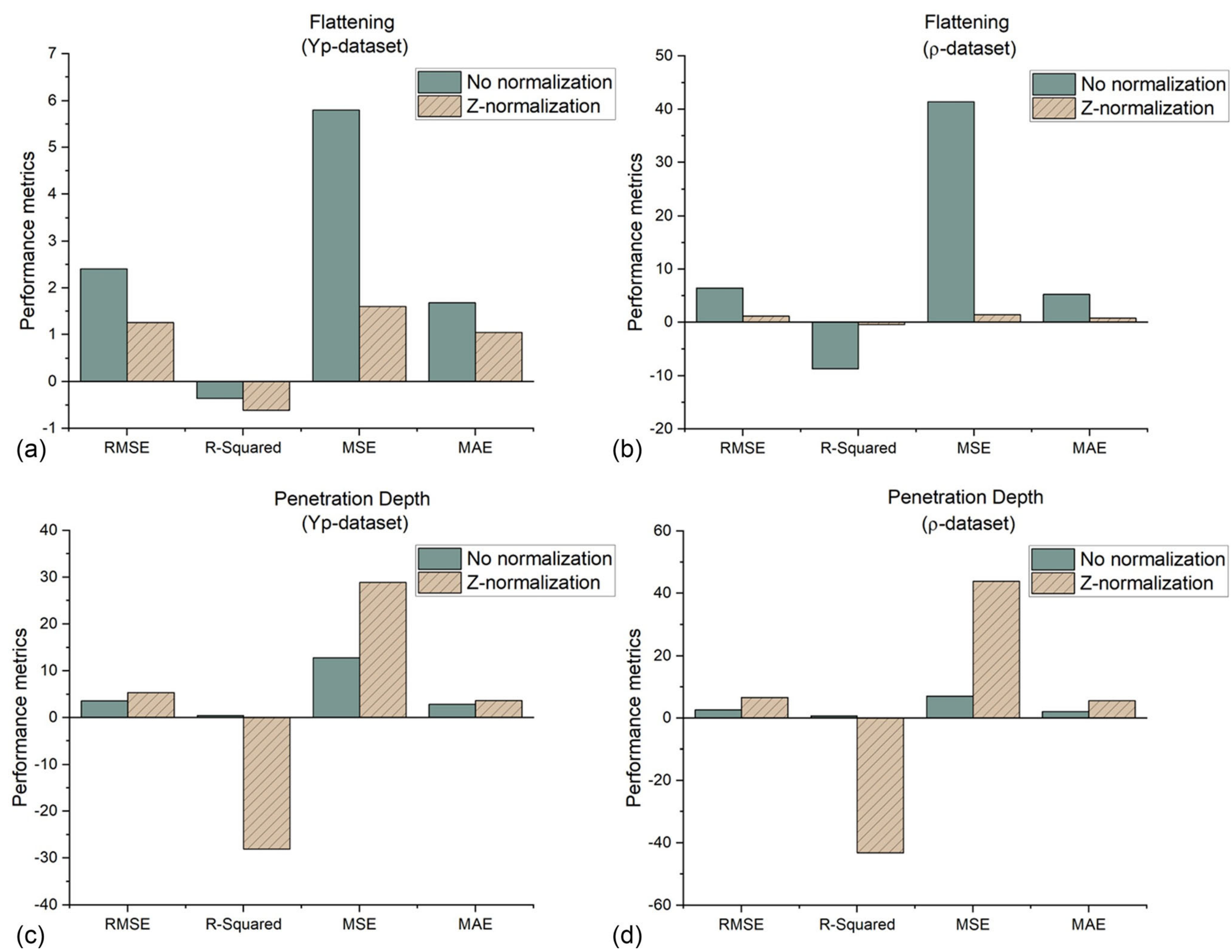

Fig. 4 Comparison of performance metrics with and without Z-score normalization for: (a) Flattening on Yp-dataset, (b) Flattening on ρ-dataset; (c) Penetration Depth on Yp-dataset; (d) Penetration Depth on ρ-dataset

flattening process where interactions between material properties and process parameters are highly nonlinear and difficult to model explicitly. In contrast, density, while less relevant for flattening, proves to be a superior input for predicting penetration depth due to its strong correlation with kinetic energy transfer. Models trained with particle density (ρ\rho$\rho$) consistently outperformed those using yield strength for penetration depth predictions, as the physical principles governing penetration depth are more directly tied to the energy transfer, which exhibits a more linear relationship with density. Boosted trees, a method based on the ensemble learning of decision trees, are better suited for capturing this type of relationship. Decision trees in a boosting framework focus on learning the residuals of previous models, allowing the model to build a piecewise approximation of the target function. This method is well-suited for capturing the linear or piecewise-linear dependencies of penetration depth on density, where the relationship can be more easily approximated by sequential binary splits that follow the inherent linearity of energy transfer processes. The application of z-score normalization improved prediction stability for by standardizing feature scales, ensuring that the models could perform more consistently by reducing the potential for one variable to dominate due to its larger magnitude, especially for the prediction of penetration depth.

To gain a deeper understanding of the relationship between the analyzed output variables and the input variables, as well as to assess better the models' ability to predict the coating characteristics after deposition, the results of the finite element simulations presented in Fig. 5 should be examined.

Figure 5 presents the flattening and penetration depth trends for the different powders analyzed. The substrates, PEEK and ABS, are characterized by high and low yield strengths, respectively, with yield strength being the only input parameter considered. To facilitate comparison, the legends in Fig. 5(a, b) are ordered by increasing yield strength, while those in Fig. 5(c, d) are arranged by increasing density.

Flattening behavior is predominantly influenced by the yield strength of the material, as particles with similar Yp values exhibit comparable trends as impact velocity changes. In contrast, for penetration depth, materials with similar density values show similar trends with varying impact velocities. This pattern holds across all substrate types; however, a distinct trend is observed at higher velocities for softer particles with lower Yp values impacting the stiffer PEEK substrate. In this case, evaluating flattening becomes more challenging due to the rigidity of the PEEK substrate, which limits the deformation of the particles. As impact velocities increase, the strain rate rises rapidly, amplifying the work-hardening effect in the material.

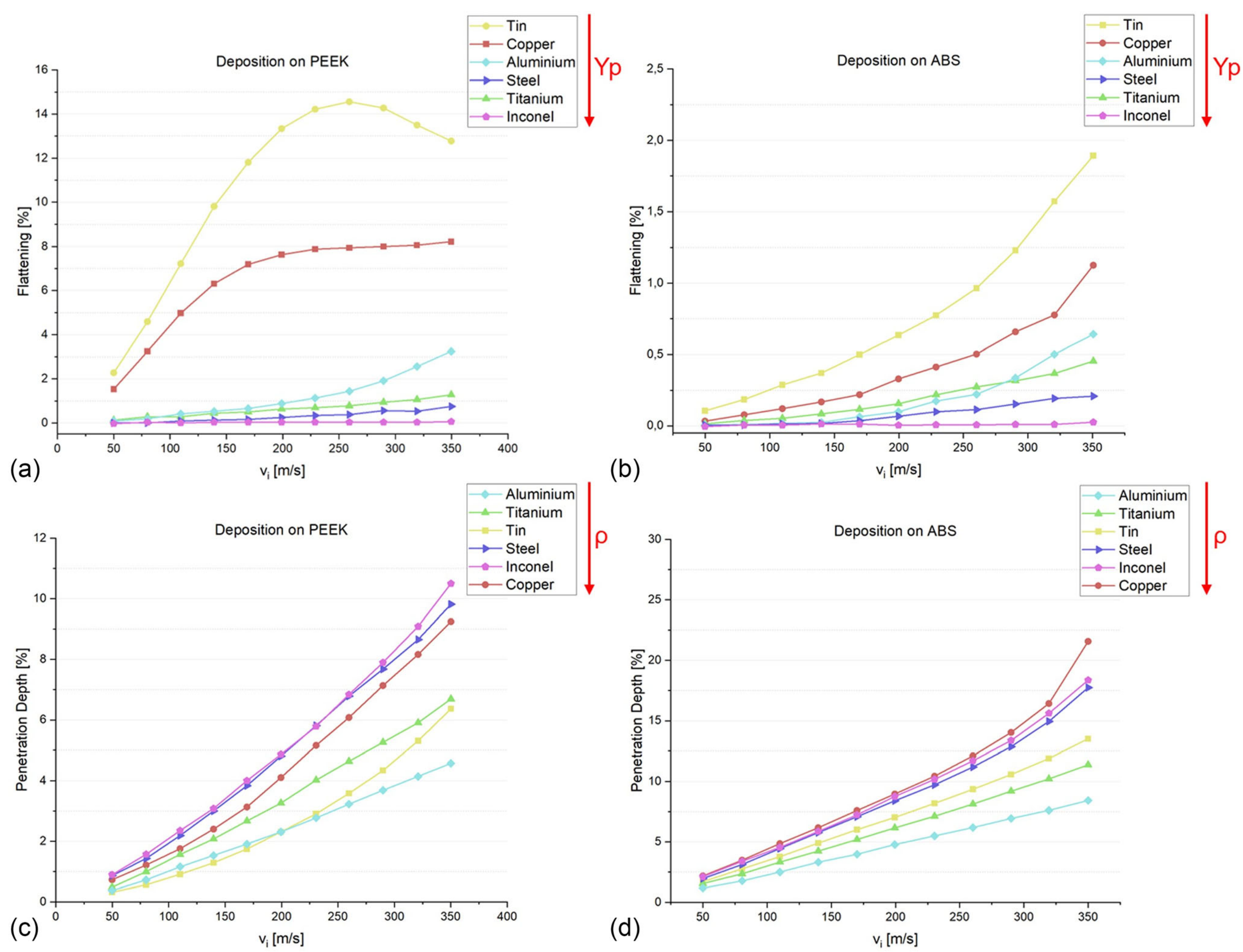

Fig. 5 Results of FEM simulations showing the effect of impact velocity on output parameters: (a) Flattening for PEEK; (b) Flattening for ABS; (c) Penetration Depth for PEEK; (d) Penetration Depth for ABS

Flattening behavior thus becomes increasingly dependent on the material properties, as softer materials experience work-hardening at lower velocities. These complex interactions make it challenging to predict flattening accurately. Therefore, further refinement of predictive models is necessary to better capture these material-dependent effects. This analysis is consistent with the results obtained from the machine learning models and highlights the crucial role of a comprehensive understanding of the underlying process when applying machine learning techniques. The accuracy of the predictions is strongly influenced by this fundamental knowledge, emphasizing the importance of a deep understanding of the process to guide and improve model development.

In conclusion, the optimization of process parameters reveals clear distinctions for maximizing flattening and penetration depth. For flattening, softer particles with low Yp, firmer substrates, and moderate impact velocities create conditions that encourage significant mechanical interlocking. In contrast, to maximize penetration depth, denser particles, softer substrates, and higher velocities are more effective, as they ensure sufficient momentum transfer and energy dissipation. The machine learning models reinforce these observations, demonstrating that Yp is crucial for predicting flattening, while ρ provides better predictions for penetration depth. Together, the engineering and computational perspectives offer a comprehensive understanding of how input parameters influence cold spraying outcomes, providing valuable insights to optimize coatings for diverse applications.

4. Conclusions

In this work, machine learning was employed in this study to identify the most influential parameters for optimizing the cold spray process for metallizing thermoplastic polymers, with a focus on powder characteristics. Two different datasets were used, one based on particle yield strength and the other on powder density, with both datasets combining experimental data and finite element modeling (FEM) simulations. The key findings from the analysis are as follows:

1. Machine learning models effectively predicted particle flattening and penetration depth, demonstrating the potential of ML to optimize the CS process for polymer coatings.
2. Different ML algorithms yielded the best performance depending on the dataset and whether normalization was applied. For example, Gaussian process regression (GPR) models showed superior performance for flattening when using the yield strength dataset with normalization, while neural networks performed better for penetration depth predictions based on the density dataset, especially when normalization was not applied. This variability emphasizes the importance of choosing the right algorithm and preprocessing method for each specific outcome.
3. The error analysis showed that the models trained on yield strength (Yp) achieved lower prediction errors for flattening, with RMSE values indicating a strong correlation between predicted and observed values. For penetration depth, models based on particle density (ρ) had slightly higher errors but still maintained a good predictive performance, demonstrating the accuracy of the approach.
4. Z-score normalization improved the stability and accuracy of the predictions, particularly for flattening. However, its impact on penetration depth predictions was less pronounced, suggesting that the effect of normalization is dependent on the specific parameter being predicted.
5. The trends observed in the ML predictions were confirmed through the analysis of FEM results. By examining the responses of different materials, it was evident that materials with similar densities exhibited similar behavior when penetration depth was plotted against impact velocity. Similarly, materials with similar yield strengths displayed comparable flattening trends. This correlation between ML predictions and FEM trends validates the reliability of the ML approach in predicting cold spray outcomes.

Acknowledgments

This study was carried out within the "OPTIMA: depOsition of cold sPray in the realm of green addiTIve manufacturing through construction of MAchine learning models" and received funding from the Research Projects of Significant National Interest (PRIN) 2022 PNRR, project n. D53D23017410001.

Author Contributions

Alessia Serena Perna: Conceptualization, Data curation, Methodology, Visualization, Writing—original draft. Alessia Auriemma Citarella: Data curation, Investigation, Fabiola De Marco: Data curation, Investigation, Luigi di Biasi: Investigation, Software; Antonio Viscusi: Software, Writing—review & editing; Tortora Genoveffa: Project administration, Supervision; Massimo Durante: Project administration, Supervision, Resources.

Funding

Open access funding provided by Università degli Studi di Napoli Federico II within the CRUI-CARE Agreement.

References

1. M. Rinaldi, M. Ferrara, L. Pigliaru, C. Allegranza, and F. Nanni, Additive Manufacturing of Polyether Ether Ketone-Based Composites for Space Application: A Mini-Review, *CEAS Space J.*, 2023, **15**(1), p 77–87
2. D.K. Yadav, R. Srivastava, and S. Dev, Design and Fabrication of ABS Part by FDM for Automobile Application, *Mater. Today Proc.*, 2020, **26**, p 2089–2093
3. M.Y. Kondo, L.S. Montagna, G.F.M. de Morgado, A.L.G. de Castilho, L.A.P.S. dos Batista, E.C. Botelho, M.L. Costa, F.R. Passador, M.C. Rezende, and M.V. Ribeiro, Recent Advances in the Use of Polyamide-Based Materials for the Automotive Industry, *Polímeros*, 2022 https://doi.org/10.1590/0104-1428.20220042
4. M.Y. Khalid, Z.U. Arif, W. Ahmed, and H. Arshad, Recent Trends in Recycling and Reusing Techniques of Different Plastic Polymers and Their Composite Materials, *Sustain. Mater. Technol.*, 2022, **31**, e00382
5. M. Grigore, Methods of Recycling Properties and Applications of Recycled Thermoplastic Polymers, *Recycling*, 2017, **2**(4), p 24
6. P. Jagadeesh, S. Mavinkere Rangappa, S. Siengchin, M. Puttegowda, S.M.K. Thiagamani, R.G.M. Hemath Kumar, O.P. Oladijo, V. Fiore, and M.M. Moure Cuadrado, Sustainable Recycling Technologies for Thermoplastic Polymers and Their Composites: A Review of the State of the Art, *Polym. Compos.*, 2022, **43**(9), p 5831–5862
7. G. Cicala, A. Latteri, B. Del Curto, A. Lo Russo, G. Recca, and S. Farè, Engineering Thermoplastics for Additive Manufacturing: A Critical Perspective with Experimental Evidence to Support Functional Applications, *J. Appl. Biomater. Funct. Mater.*, 2017, **15**(1), p 10–18
8. A.S. Rahate, K.R. Nemade, and S.A. Waghuley, Polyphenylene Sulfide (PPS): State of the Art and Applications, *Rev. Chem. Eng.*, 2013 https://doi.org/10.1515/revce-2012-0021
9. I. Gouzman, E. Grossman, R. Verker, N. Atar, A. Bolker, and N. Eliaz, Advances in Polyimide-Based Materials for Space Applications, *Adv. Mater.*, 2019 https://doi.org/10.1002/adma.201807738
10. H.F. Brinson and L.C. Brinson, *Polymer Engineering Science and Viscoelasticity*, Springer, US, Boston, 2008
11. J.M. Henshaw, V. Wood, and A.C. Hall, Failure of Automobile Seat Belts Caused by Polymer Degradation, *Eng. Fail. Anal.*, 1999, **6**(1), p 13–25
12. R. Melentiev, A. Yudhanto, R. Tao, T. Vuchkov, and G. Lubineau, Metallization of Polymers and Composites: State-of-the-Art Approaches, *Mater. Des.*, 2022, **221**, 110958
13. K. Gautam, D. Gogoi, T.D. Kongnyui, S. Devi, C. Kumar, and M. Kumar, A Comprehensive Review on Surface Modifications of Polymer-based 3D-printed Structures: Metal Coating Prospects and Challenges, *Polym. Adv. Technol.*, 2024 https://doi.org/10.1002/pat.6369
14. A. Moridi, S.M. Hassani-Gangaraj, M. Guagliano, and M. Dao, Cold Spray Coating: Review of Material Systems and Future Perspectives, *Surf. Eng.*, 2014, **30**(6), p 369–395. https://doi.org/10.1179/1743294414Y.0000000270
15. P. Panjan, A. Drnovšek, P. Gselman, M. Čekada, and M. Panjan, Review of Growth Defects in Thin Films Prepared by PVD Techniques, *Coatings*, 2020, **10**(5), p 447
16. R. Della Gatta, A.S. Perna, A. Viscusi, G. Pasquino, and A. Astarita, Cold Spray Deposition of Metallic Coatings on Polymers: A Review, *J. Mater. Sci.*, 2021, **57**, p 27
17. J.-T. Tsai, M.B.-G. Jun, and D.F. Bahr, Adhesion of Rough Cold Sprayed Metal Coatings on Polymers, *Surf. Eng.*, 2023, **39**(2), p 161–173
18. A. Papyrin, The Development of the Cold Spray Process, *The Cold Spray Materials Deposition Process*. Elsevier, 2007, p 11–42. https://doi.org/10.1533/9781845693787.1.11
19. A. Małachowska, L. Pawłowski, M. Winnicki, T. Piasecki, A. Ambroziak, The Possibility of Cold Spray Process Application to Obtain Electrically Conductive Coatings on Polymers, in *ITCS 2015—Proceedings of the International Thermal Spray Conference*, (2015)
20. A. Viscusi, A.S. Perna, and A. Astarita, A Preliminary Study on the Sustainability of Metallization of Polymer Matrix Composites through Cold Spray, *J. Mater. Eng. Perform.*, 2023, **32**, p 3888
21. H. Che, X. Chu, P. Vo, and S. Yue, Metallization of Various Polymers by Cold Spray, *J. Therm. Spray Technol.*, 2018, **27**(1–2), p 169–178
22. A. Sturgeon, B. Dunn, S. Celotto, and W. O'Neill, Cold Sprayed Coatings for Polymer Composite Substrate, *ESA SP*, 2006, **616**(1), p 1–5
23. R. Della Gatta, A. Viscusi, A.S. Perna, A. Caraviello, and A. Astarita, Feasibility of Steel Powder Deposition on Composites through Cold Spray, *Mater. Manuf. Process.*, 2021, **36**(3), p 281
24. H. Che, M. Gagné, P.S.M. Rajesh, J.E. Klemberg-Sapieha, F. Sirois, D. Therriault, and S. Yue, Metallization of Carbon Fiber Reinforced Polymers for Lightning Strike Protection, *J. Mater. Eng. Perform.*, 2018, **27**(10), p 5205–5211
25. B. Karahan, I. Ozdemir, T. Grund, N. Hanisch, and T. Lampke, Advancements in Cold Spraying for Polymer Matrix Composites: Enhanced LSP and EMI Shielding Performance—Review and Future Directions, *J. Mater. Sci. Mater. Eng.*, 2025, **20**(1), p 13
26. K. Koser, S. Kousar, S. Haider, S. Khan, A.A. Bhat, and A.A. Hashmi, Functional Coatings: Innovation and Challenges; Coatings in Biological Systems, *Functional Coatings for Biomedical, Energy, and Environmental Applications*. R.K. Arya, G.D. Verros, J. Paulo Davim Ed., Wiley, 2024, p 31–50
27. A.S. Alhulaifi, G.A. Buck, and W.J. Arbegast, Numerical and Experimental Investigation of Cold Spray Gas Dynamic Effects for Polymer Coating, *J. Therm. Spray Technol.*, 2012, **21**(5), p 852–862
28. A. Heydari Astaraee, C. Colombo, and S. Bagherifard, Numerical Modeling of Bond Formation in Polymer Surface Metallization Using Cold Spray, *J. Therm. Spray Technol.*, 2021, **30**(7), p 1765–1776
29. K. Malamousi, K. Delibasis, B. Allcock, and S. Kamnis, Digital Transformation of Thermal and Cold Spray Processes with Emphasis on Machine Learning, *Surf. Coat. Technol.*, 2022, **433**, p 128138
30. H. Canales, I.G. Cano, and S. Dosta, Window of Deposition Description and Prediction of Deposition Efficiency via Machine Learning Techniques in Cold Spraying, *Surf. Coat. Technol.*, 2020, **401**, p 126143. https://doi.org/10.1016/j.surfcoat.2020.126143
31. J. Cai, J. Luo, S. Wang, and S. Yang, Feature Selection in Machine Learning: A New Perspective, *Neurocomputing*, 2018, **300**, p 70–79
32. F. Gärtner, T. Stoltenhoff, T. Schmidt, and H. Kreye, The Cold Spray Process and Its Potential for Industrial Applications, *J. Therm. Spray Technol.*, 2006, **15**, p 223
33. A.S. Perna, A. Viscusi, R. Della Gatta, and A. Astarita, Cold Spraying on Polymer-Based Composites: Understanding the Single-Particle Adhesion, *Surf. Coat. Technol.*, 2022, **447**, p 128837
34. S.V. Klinkov, V.F. Kosarev, and M. Rein, Cold Spray Deposition: Significance of Particle Impact Phenomena, *Aerosp. Sci. Technol.*, 2005, **9**(7), p 582–591
35. H. Parmar, F. Tucci, P. Carlone, and T.S. Sudarshan, Metallisation of Polymers and Polymer Matrix Composites by Cold Spray: State of the Art and Research, *Perspectives*, 2021 https://doi.org/10.1080/09506608.2021.1954805
36. A.A. Tiamiyu and C.A. Schuh, Particle Flattening during Cold Spray: Mechanistic Regimes Revealed by Single Particle Impact Tests, *Surf. Coat. Technol.*, 2020, **403**, 126386
37. P.C. King, A.J. Poole, S. Horne, R. de Nys, S. Gulizia, and M.Z. Jahedi, Embedment of Copper Particles into Polymers by Cold Spray, *Surf. Coat. Technol.*, 2013, **216**, p 60–67
38. D. Garcia-Gonzalez, A. Rusinek, T. Jankowiak, and A. Arias, Mechanical Impact Behavior of Polyether-Ether-Ketone (PEEK), *Compos. Struct.*, 2015, **124**, p 88–99
39. Q. Wang, X. Luo, S. Tsutsumi, T. Sasaki, C. Li, and N. Ma, Measurement and Analysis of Cold Spray Residual Stress Using Arbitrary Lagrangian-Eulerian Method, *Addit. Manuf.*, 2020, **35**, 101296
40. C.R. Rao and H. Toutenburg, Linear Models, *Linear Models*. Springer New York, New York, 1995, p 3–18. https://doi.org/10.1007/978-1-4899-0024-1_2
41. O. Maimon and L. Rokach Eds., *Data Mining and Knowledge Discovery Handbook, (Boston, MA)*, Springer, US, 2010
42. T.G. Dietterich, Ensemble Methods in Machine Learning, *Multiple Classifier Systems*. Springer Berlin Heidelberg, Berlin, Heidelberg, 2000, p 1–15. https://doi.org/10.1007/3-540-45014-9_1
43. M.A. Hearst, S.T. Dumais, E. Osuna, J. Platt, and B. Scholkopf, Support Vector Machines, *IEEE Intel. Syst. Appl.*, 1998, **13**(4), p 18–28
44. A. Viscusi, M. Bruno, L. Carrino, R. Della Gatta, G. Iandolo, and A.S. Perna, Study of Bonding Mechanisms in Cold Spray of Metal-to-Polymer through a Numerical Approach, *Key Eng. Mater.*, 2022, **926**, p 56–64

45. A. Fardan, C.C. Berndt, and R. Ahmed, Numerical Modelling of Particle Impact and Residual Stresses in Cold Sprayed Coatings: A Review, *Surf. Coat. Technol.*, 2021, **409**, 126835
46. L. Boccarusso, G. Arleo, A. Astarita, F. Bernardo, P. De Fazio, M. Durante, F.M.C. Minutolo, R. Sepe, and A. Squillace, A New Approach to Study the Influence of the Weld Bead Morphology on the Fatigue Behaviour of Ti-6Al-4V Laser Beam-Welded Butt Joints, *Int. J. Adv. Manuf. Technol.*, 2017, **88**, p 75–88
47. A. Formisano, L. Carrino, D. De Fazio, M. Durante, and A. Viscusi, Enhanced Aluminium Foam Based Cylindrical Sandwiches: Bending Behaviour and Numerical Modeling, *Int. Rev. Model. Simul. (IREMOS)*, 2018, **11**(4), p 198–205
48. H. Unal and A. Mimaroglu, Friction and Wear Characteristics of PEEK and Its Composite under Water Lubrication, *J. Reinforc. Plast. Comp. Sage Public. CA Thous. Oaks CA*, 2006, **25**(16), p 1659–1667
49. R. Della Gatta, A. Viscusi, A.S. Perna, A. Caraviello, and A. Astarita, Cold Spray Process for the Production of AlSi10Mg Coatings on Glass Fibers Reinforced Polymers, *Mater. Manuf. Process.*, 2021, **36**(1), p 106
50. L. Alonso, M.A. Garrido-Maneiro, and P. Poza, A Study of the Parameters Affecting the Particle Velocity in Cold-Spray: Theoretical Results and Comparison with Experimental Data, *Addit. Manuf.*, 2023, **67**, 103479
51. M. Grujicic, C.L. Zhao, C. Tong, W.S. DeRosset, and D. Helfritch, Analysis of the Impact Velocity of Powder Particles in the Cold-Gas Dynamic-Spray Process, *Mater. Sci. Eng. A*, 2004, **368**(1–2), p 222–230
52. R.N. Raoelison, E. Aubignat, M.-P. Planche, S. Costil, C. Langlade, and H. Liao, Low Pressure Cold Spraying under 6 Bar Pressure Deposition: Exploration of High Deposition Efficiency Solutions Using a Mathematical Modelling, *Surf. Coat. Technol.*, 2016, **302**, p 47–55
53. L. Lalu Khoitara, R.N. Raoelison, and S. Costil, 60% IACS Conductive Metal Coating on a Polymer Surface: Achievement of a Highly Efficient Additive Processing by Cold Spraying, *Powders*, 2022, **1**(4), p 262–272
54. T. Zhang, E. Padayodi, I. Goda, J.-C. Sagot, and R.N. Raoelison, Development of an Epoxy-Metallic Powder Sublayer for the Cold Spray Metallization of Carbon-Fiber Reinforced Thermoset Composites, *Results Surf. Interfaces*, 2025, **18**, 100373
55. A.S. Perna, A. Viscusi, R. Della Gatta, and A. Astarita, Integrating 3D Printing of Polymer Matrix Composites and Metal Additive Layer Manufacturing: Surface Metallization of 3D Printed Composite Panels through Cold Spray Deposition of Aluminium Particles, *Int. J. Mater. Form.*, 2022, **15**(2), p 15. https://doi.org/10.1007/S12289-022-01665-9
56. M. Chen, H. Che, and S. Yue, Exploring Surface Preparation for Cold Spraying on Polymers, *Surf. Coat. Technol.*, 2022, **450**, 128993
57. A. Viscusi, A.S. Perna, A. Astarita, L. Boccarusso, A. Caraviello, L. Carrino, R.D. Gatta, M. Durante, and R. Sansone, Experimental Study of Cold Sprayed Metallic Coatings on Thermoplastic Matrix Composites, *Key Eng. Mater.*, 2019, **813**, p 68–73. https://doi.org/10.4028/www.scientific.net/KEM.813.68
58. A. Viscusi, A. Astarita, D. Borrelli, A. Caraviello, L. Carrino, R.D. Gatta, V. Lopresto, I. Papa, A.S. Perna, R. Sansone, and A. Squillace, On the Influence of Manufacturing Strategy of 3D-Printed Polymer Substrates on Cold Spray Deposition, *ESAFORM 2021*, 2021 https://doi.org/10.25518/esaform21.3003
59. A. Viscusi, M. Durante, A. Astarita, L. Boccarusso, L. Carrino, and A.S. Perna, Experimental Evaluation of Metallic Coating on Polymer by Cold Spray, *Proc. Manuf.*, 2020, **47**, p 761
60. M.R. Rokni, P. Feng, C.A. Widener, and S.R. Nutt, Depositing Al-Based Metallic Coatings onto Polymer Substrates by Cold Spray, *J. Therm. Spray Technol.*, 2019, **28**, p 1699
61. H. Che, P. Vo, and S. Yue, Investigation of Cold Spray on Polymers by Single Particle Impact Experiments, *J. Therm. Spray Technol.*, 2019, **28**(1–2), p 135–143
62. C. Chen, X. Xie, Y. Xie, X. Yan, C. Huang, S. Deng, Z. Ren, and H. Liao, Metallization of Polyether Ether Ketone (PEEK) by Copper Coating via Cold Spray, *Surf. Coat. Technol.*, 2018, **342**, p 209–219
63. H. Abdi, *Z-Scores Encyclopedia of measurement and statistics*, Sage Publishing Thousand Oaks, California, 2007

Publisher's Note Springer Nature remains neutral with regard to jurisdictional claims in published maps and institutional affiliations.